Am J Transl Res 2025;17(1):634-644
www.ajtr.org /ISSN:1943-8141/AJTR0161050

Original Article

Sodium fluoride accelerates apoptosis, oxidative stress and matrix degradation of condylar chondrocytes by upregulating MMP-13 and RANKL

Xiangwen Zhou[1], Wei Zu[1], Lian Zhao[2], Xiaojiao Gong[2], Qingsong Jiang[1]

[1]Department of Prosthodontics, Beijing Stomatological Hospital, Capital Medical University, Beijing 100050, China; [2]Department of Prosthodontics, Hospital of Stomatology, Zunyi Medical University, Zunyi 563000, Guizhou, China

Received October 10, 2024; Accepted December 28, 2024; Epub January 15, 2025; Published January 30, 2025

Abstract: Objective: To explore the regulatory effects of sodium fluoride (NaF) exposure on apoptosis, oxidative stress, and matrix degradation in condylar chondrocytes and subchondral osteoblasts using *in vitro* and *in vivo* experiments. Methods: Condylar chondrocytes and subchondral osteoblasts were treated with 5 mg/L and 50 mg/L NaF, respectively, and cell viability was detected. Chondrocyte apoptosis was detected by flow cytometry and western blotting. Oxidative stress, inflammatory factor secretion, and cell matrix degradation were detected using specific kits. RT-qPCR was used to detect the expression of osteoblast phenotype genes. A rat model of fluorosis was established to study the effects of fluoride exposure on condylar cartilage and subchondral bone *in vivo*. Results: Low concentration of NaF enhanced the activity of chondrocytes and osteoblasts, but high concentration of NaF inhibited cell activity. Fluoride exposure induced chondrocyte apoptosis, oxidative stress, inflammatory response, and matrix degradation. It also decreased the expression of osteoblast phenotype gene osteoprotegerin (OPG) and increased the expression of osteoclast phenotype gene receptor activator of nuclear factor κB ligand (RANKL). In fluorosis rats, urinary and bone fluoride levels were increased, cartilage damage was aggravated, and the number of osteoclasts in subchondral bone was increased. Conclusion: Fluoride exposure induces pathologic changes in condylar cartilage and subchondral bone in rats, possibly by upregulation of matrix metalloproteinase-13 (MMP-13) and RANKL.

Keywords: Temporomandibular disorder, fluorine, condylar chondrocytes, subchondral osteoblasts, injury

Introduction

Fluorine, which is widely distributed in nature, is one of the trace elements necessary for human metabolism [1]. It is primarily absorbed through water, food and air, and is predominantly stored in bones and teeth. A moderate amount of fluorine can strengthen bones and prevent tooth decay [2]. However, environmental deterioration has led to a significant increase in fluorine levels in water, food, and air. Eventually, excessive fluoride accumulates in the body and triggers many chronic diseases [3]. When the onset of these diseases is confined to specific places, it is called endemic fluorosis. Underground water is considered a major source of endemic fluorosis [4]. Despite global efforts to reduce fluoride levels in water, endemic fluorosis remains prevalent in 40 countries worldwide, including China [5]. Therefore, endemic fluorosis has become an urgent public concern that needs solutions [6].

Injuries due to fluorosis are categorized into dental, skeletal, and non-skeletal injuries [7]. Dental fluorosis is the earliest and most common manifestation of the condition. Excessive fluoride absorption into the enamel inhibits ameloblast proliferation, impairing enamel mineralization. This leads to the formation of enamel plaques, which can range from chalky white to brown, and may result in defects in newly erupted teeth [8, 9]. The disease not only affects appearance but also imposes a psychological burden.

Fluorine-induced bone damage, also known as skeletal fluorosis, is a chronic and aggressive

https://doi.org/10.62347/NIIL5728

disease that affects bones, cartilage, and joints. It is characterized by pathologic changes such as osteosclerosis, osteochondrosis, osteoporosis, and heterotopic ossification. In the early stages, symptoms such as persistent pain, joint stiffness, and limited movement in the joints, spine, and extremities are common. As the disease progresses, these conditions worsen, eventually leading to physical deformities and, in severe cases, paralysis [10].

The temporomandibular joint (TMJ) consists of condylar processes of the jaws, articular surfaces of the temporal bone, articular disc, the surrounding joint capsule, and articular ligaments. As the only movable joint in the maxillofacial region, the TMJ plays a key role in opening and closing the mouth and in mastication. Damage to the TMJ structure and initiation of pathological changes can lead to temporomandibular disorder (TMD), which manifests as pain, clicking and even movement dysfunction [11]. It was reported that patients with skeletal fluorosis also showed symptoms of temporomandibular joint disorder, resembling TMD [12]. As the main bone structure of the temporomandibular joint, the condylar process is involved in the growth and development of the mandible through endochondral ossification. Fibrocartilage covers its surface, serving as the functional area of the joint, and this region is often the first to be affected by joint diseases. As secondary cartilage, it has a remarkable capacity for growth and regeneration when affected by external factors. Degeneration of articular cartilage of the condyles and resorption of subchondral bone frequently occur in patients with TMD. This raises the question of whether fluoride, which induces bone damage, can also affect the condylar cartilage and bone, contributing to the progression of TMD or whether its regulatory mechanism differs from that seen in skeletal fluorosis.

Currently, there is limited research on the effects of fluoride on the TMJ and condylar process. In this study, we targeted the condylar process to investigate the effects of fluorine at different concentrations on condylar cartilage and bones using both *in vivo* and *in vitro* experiments. Meanwhile, we used molecular biologic techniques to explore the underlying mechanism and identify target genes. The goal is to provide experimental references for clarifying the correlation between fluorine exposure and the development of TMD, offering insight into the etiology of TMD and potential avenues for treatment.

Materials and methods

Modeling rats with fluorosis

Fifteen 3-week-old specific pathogen-free (SPF) male Sprague Dawley (SD) rats weighing 60 ± 10 g were randomly selected for this study. The rats were housed at the Experimental Animal Center of Beijing Stomatological Hospital, School of Stomatology, Capital Medical University. After one week of acclimatization, the rats were randomly divided into a low-fluoride (LF) group, a high-fluoride (HF) group and a control group, with 5 rats in each group. Rats in the control group, LF group and HF group were given deionized water, sodium fluoride (NaF, Sigma-Aldrich) solution (5 mg/L) and NaF solution (50 mg/L), respectively. Three months later, varying degrees of dental fluorosis were observed in rats from the LF and HF groups. The rats were euthanized by cervical dislocation, and bilateral condylar processes were collected for morphologic observation. All animal procedures conformed to the laboratory animal guidelines, and the study was approved by the Ethics Committee for Animal Experiments of Beijing Stomatological Hospital, School of Stomatology, Capital Medical University.

Hematoxylin (H&E) staining

The condylar processes were fixed in 4% paraformaldehyde solution for 24 hours, followed by decalcification in JYBI-I decalcification solution. After 24-36 h, the condylar processes were dehydrated with gradient alcohol, embedded with paraffin, sliced and stained with HE (Sigma-Aldrich, St. Louis, Missouri). For quantitative analysis, images of the H&E-stained sections were captured using a light microscope (Olympus IX71; Tokyo, Japan) equipped with a digital camera at ×200 magnification. A minimum of five non-overlapping fields per slide from three independent animals were randomly selected from each experimental group to minimize sampling bias. Image analysis was conducted using ImageJ, an open-source image processing program. Additionally, positive-stained areas were segmented based on predefined thresholds, and the percentage of posi-

tively stained tissue relative to the total tissue area was calculated.

Tartrate-resistant acid phosphatase (TRAP) staining

After dewaxing, the slices were washed 3 times with water and distilled water followed with incubation in TRAP staining solution at 37°C for 20 minutes. Then, the dyes were discarded, and the slices were washed with water and counterstained with HE. Afterward, the slices were dehydrated and sealed. For quantitative analysis of TRAP-positive cells, images were captured using a light microscope (Zeiss, Germany) equipped with a digital camera at ×200 magnification. A minimum of five random non-overlapping fields per slide from three independent experiments were analyzed to ensure representativeness. TRAP-positive multinucleated cells containing more than three nuclei were counted as osteoclasts.

Primary chondrocyte culture and identification

The bilateral condylar articular cartilage of healthy 3-week-old SD rats was obtained under sterile conditions for chondrocytes isolation and culture. The tissue was cut into 1 mm^3 pieces and digested with 0.25% trypsin at 37°C for 10 min. After removing the trypsin, 0.2% type II collagenase was added, and the tissues were incubated at 37°C for 2 h. The supernatant was collected every 1 h. Then, DMEM F-12 (Gibco, New York, USA) was added to terminate digestion. Afterward, the tissues were centrifuged (1000 rounds per min) for 5 min. The resulting cell pellet was collected and resuspended. The cells were inoculated in a culture bottle (25 cm^2) at a density of 2×10^5 cells per well under the condition of 5% carbon dioxide (CO_2) at 37°C. The fluid was replaced every 2 days (d). The cells were passaged at a ratio of 1:2 when they reached 85%-90% confluence. The second-generation cells were collected and characterized by immunofluorescence for type II collagen and toluidine blue staining to confirm chondrocyte identity.

Primary osteoblast culture and identification

The bilateral subchondral bones of condyles from healthy 3-week-old SD rats were obtained under sterile conditions for osteoblast isolation and culture. The tissues were washed 3 times with PBS containing 1% dual antibody. Then, they were cut into 1 mm^3 pieces and placed in a culture bottle (25 cm^2) coated with serum. Then, the bottle was inverted in an incubator at 37°C with 5% CO_2 for 2 h. L-DMEM (3 mL) was subsequently added, and the bottle was set upright for continued incubation. The medium was replaced every 2 d. When the cells reached 85%-90% confluence, they were passaged at a 1:2 ratio. Purification of osteoblasts was achieved using differential attachment. The second-generation cells were collected and characterized by alizarin red staining for mineralization and alkaline phosphatase (ALP) staining for osteoblast differentiation.

Cell Counting Kit-8 (CCK-8) assay

Chondrocytes and osteoblasts were seeded at 1×10^4 cells/well in 96-well plates. Cell viability was assessed at 24, 48, and 72 h after transfection using CCK-8 assay (Dojindo, Kumamoto, Japan). To measure cell viability, the culture supernatant was discarded, and 100 μL of CCK-8 solution was added to each well. The cells were incubated in a 37°C incubator for 4 h, and the absorbance at 450 nm was measured using a microplate reader.

Flow cytometry

Cells were collected and rinsed 3 times with PBS to remove residual medium. A cell suspension (1×10^6 cells/mL) was prepared and transferred to a culture tube. Annexin V-FITC (Lianke Biotechnology, Hangzhou, China) and propidium iodide were added to the culture tube and incubated in the dark for 20 min. After incubation, binding buffer was added to the tube, and apoptosis was detected using flow cytometry (BD Biosciences, USA).

Western blotting

Total protein was extracted from cells using RIPA lysis buffer. The proteins were transferred to polyvinylidene fluoride (PVDF, Bio-Rad, Hercules, CA, USA) membranes and blocked for 2 h at room temperature. The membranes were incubated with primary antibodies (Abcam, UK) overnight at 4°C. The primary antibodies included glyceraldehyde-3-Phosphate Dehydrogenase (GAPDH, 1:1000, ab8245, Abcam), cleaved caspase3 (1:1000, ab2302, Abcam) and B-cell Lymphoma 2 (Bcl-2, 1:1500, ab32124, Abcam).

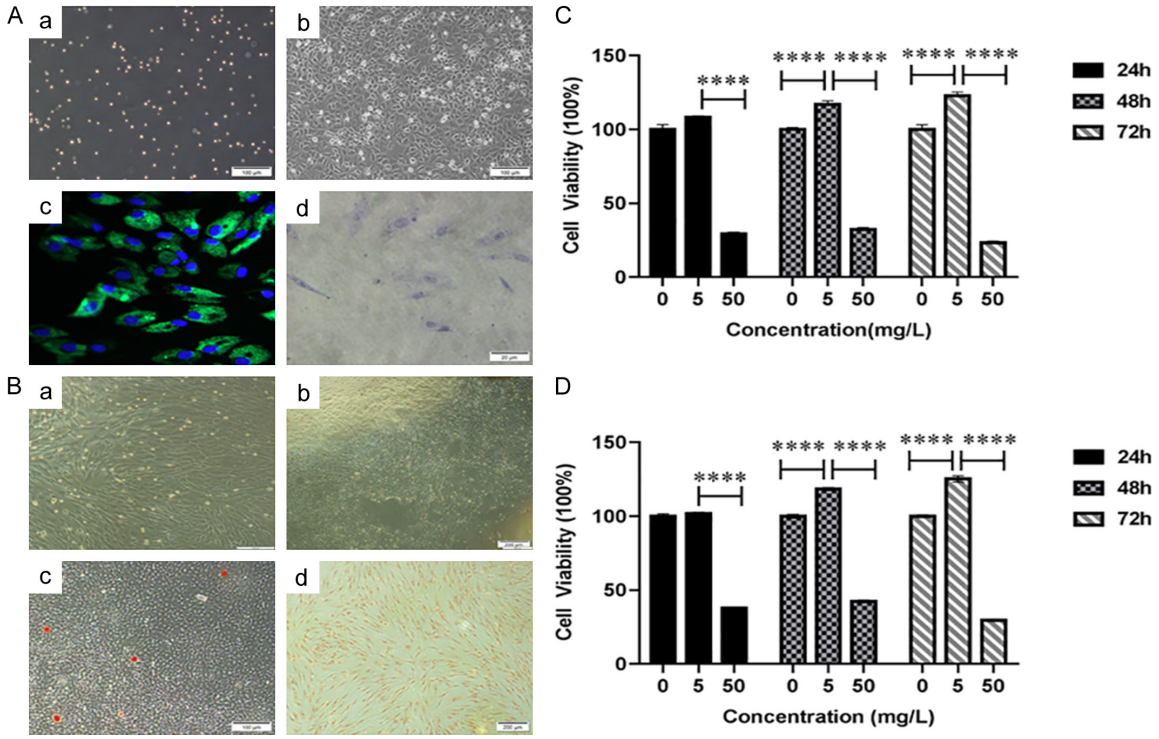

Figure 1. Effect of fluoride exposure on the cell viability of chondrocytes and osteoblasts. A. a. Cellular culture of chondrocytes at 0 d; b. Cellular culture of chondrocytes at 5 d; c. Type II collagen immunofluorescence staining of chondrocytes; d. Toluidine blue staining of chondrocytes. B. a. Cellular culture of osteoblasts at 3 d; b. Cellular culture of osteoblasts at 5 d; c. Alizarin red staining of osteoblasts; d. Alkaline phosphatase staining of osteoblasts. C. Cell viability of chondrocytes. D. Cell viability of osteoblasts. N=3. ****P<0.01.

Then, the membranes were incubated with secondary antibodies (goat anti-rabbit IgG, 1:3000, ab6721, Abcam) for 1 h at room temperature. The protein bands were visualized using enhanced chemiluminescence reagents, and densitometric analysis was performed using ImageJ software (National Institutes of Health, Bethesda, MD, USA).

Enzyme-Linked Immunosorbent Assay (ELISA)

The secretion levels of interleukin-6 (IL-6), tumor necrosis factor-α (TNF-α), and cyclooxygenase-2 (COX-2) in cell culture supernatants were detected using ELISA kits (Sigma). Additionally, the secretion levels of matrix metalloproteinase-9 (MMP9), MMP13, Collagen II, and A disintegrin and metalloproteinase with thrombospondin motifs 5 (ADAMTS5) were detected using corresponding detection kits (Sigma, St. Louis, MO, USA) according to the manufacturer's instructions.

Statistical analyses

All statistical analyses were performed using SPSS software (version 20.0; SPSS, Chicago, IL, USA). Quantitative data derived from three independent experiments were expressed as mean ± standard deviation (Mean ± SD). The normality of the data was assessed using the Shapiro-Wilk test, and homogeneity of variance was verified with Levene's test. Comparisons between multiple groups were conducted using ANOVA with a Least-Significant Difference (LSD) test. P<0.05 indicated statistical significance.

Results

Fluoride exposure inhibits the viability of chondrocytes and osteoblasts

Primary chondrocytes were round with strong refractive properties (**Figure 1A-a**). After 5 days of culture, the chondrocytes formed triangles or polygons, while the nuclei were round or oval (**Figure 1A-b**). Immunofluorescence staining for type II collagen confirmed the identification of chondrocytes, with the cell membrane and cytoplasm staining green, and the nucleus blue (**Figure 1A-c**). Toluidine blue staining showed blue cytoplasm and indigo blue nucleus (**Figure 1A-d**). For osteoblasts, initial cultures on day 3

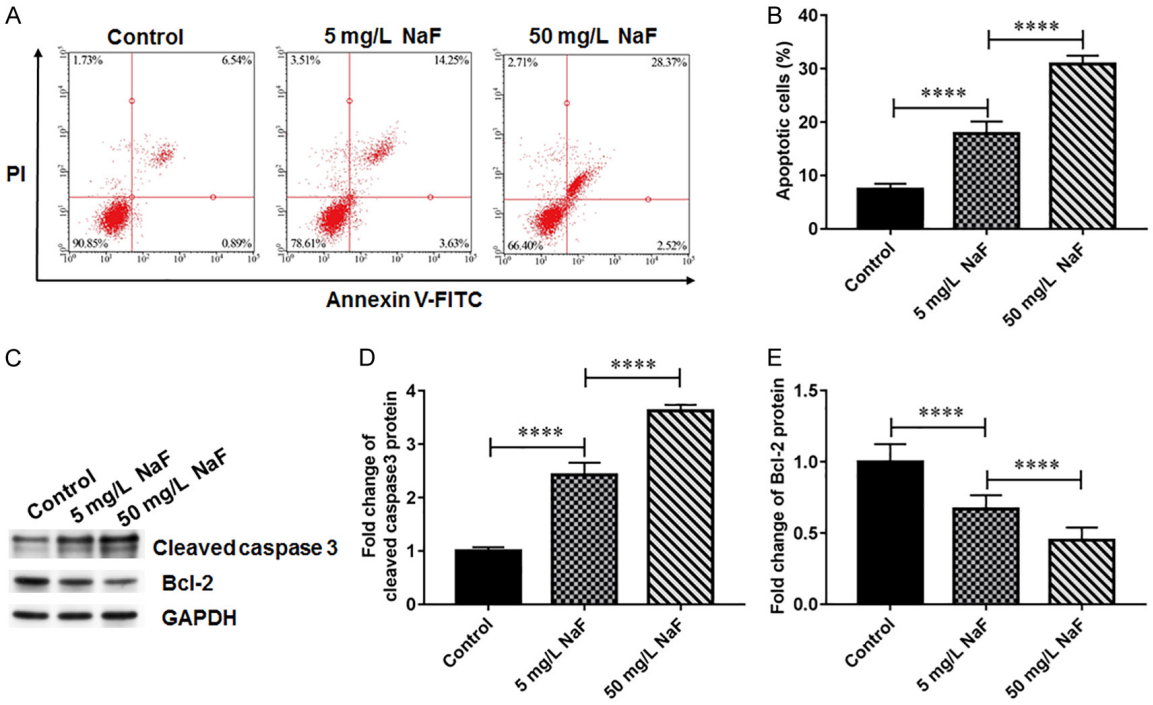

Figure 2. Effect of fluoride exposure on chondrocyte apoptosis. Chondrocytes were exposed to NaF solution (5 mg/L and 50 mg/L). A, B. Cell apoptosis (flow cytometry). C-E. Protein expression of Cleaved caspase 3 and B-cell Lymphoma 2 (Bcl-2) (western blotting). N=3. ****P<0.01.

showed some cell adhesion and spindle-shaped or polygonal osteoblasts (**Figure 1B-a**). By day 7, the cells fused and spread to the bottom of the culture dish, exhibiting a characteristic "running water" pattern (**Figure 1B-b**). Alizarin red staining revealed some red mineralized nodules of varying sizes (**Figure 1B-c**), and alkaline phosphatase staining showed positive staining in particles within the cell membrane and cytoplasm (**Figure 1B-d**). CCK-8 assay showed that low concentrations of fluoride enhanced the viability of both chondrocytes (**Figure 1C**) and osteoblasts (**Figure 1D**) after 48 and 72 h exposure. However, the viability of cells exposed to high concentrations of fluoride was significantly reduced compared to the low-concentration group.

Fluoride exposure promoted chondrocyte apoptosis

Chondrocytes exposed to NaF solution at concentrations of 5 mg/L and 50 mg/L showed an increase in apoptosis. The number of apoptotic cells was significantly higher in the high-concentration NaF group compared to the low-concentration group (**Figure 2A**, **2B**). Western blot analysis revealed that exposure to NaF led to increased expression of cleaved caspase-3, a marker of apoptosis (**Figure 2C**, **2D**), while the anti-apoptotic protein Bcl-2 was downregulated (**Figure 2C**, **2E**). These results suggest that fluoride exposure induces chondrocyte apoptosis in a dose-dependent manner.

Fluoride exposure promoted oxidative stress and inflammatory response in chondrocytes

As shown in **Figure 3A**, compared to the control group, the malondialdehyde (MDA) content in the fluoride-exposed chondrocytes elevated significantly, with higher MDA levels observed as the fluoride dose increased. This indicates that excessive fluoride exposure induces lipid peroxidation of chondrocytes (**Figure 3A**). In terms of antioxidant activity, the levels of total antioxidant capacity (T-AOC) (**Figure 3B**), the activities of total superoxide dismutase (T-SOD) (**Figure 3C**), and glutathione peroxidase (GSH-PX) (**Figure 3D**) in chondrocytes of fluoride-exposure groups were significantly lower than those of the control group. The decrease in these antioxidant markers was dose-dependent, suggesting that fluoride exposure reduced the antioxidant capacity of chondrocytes. In addition, compared to the control group, both

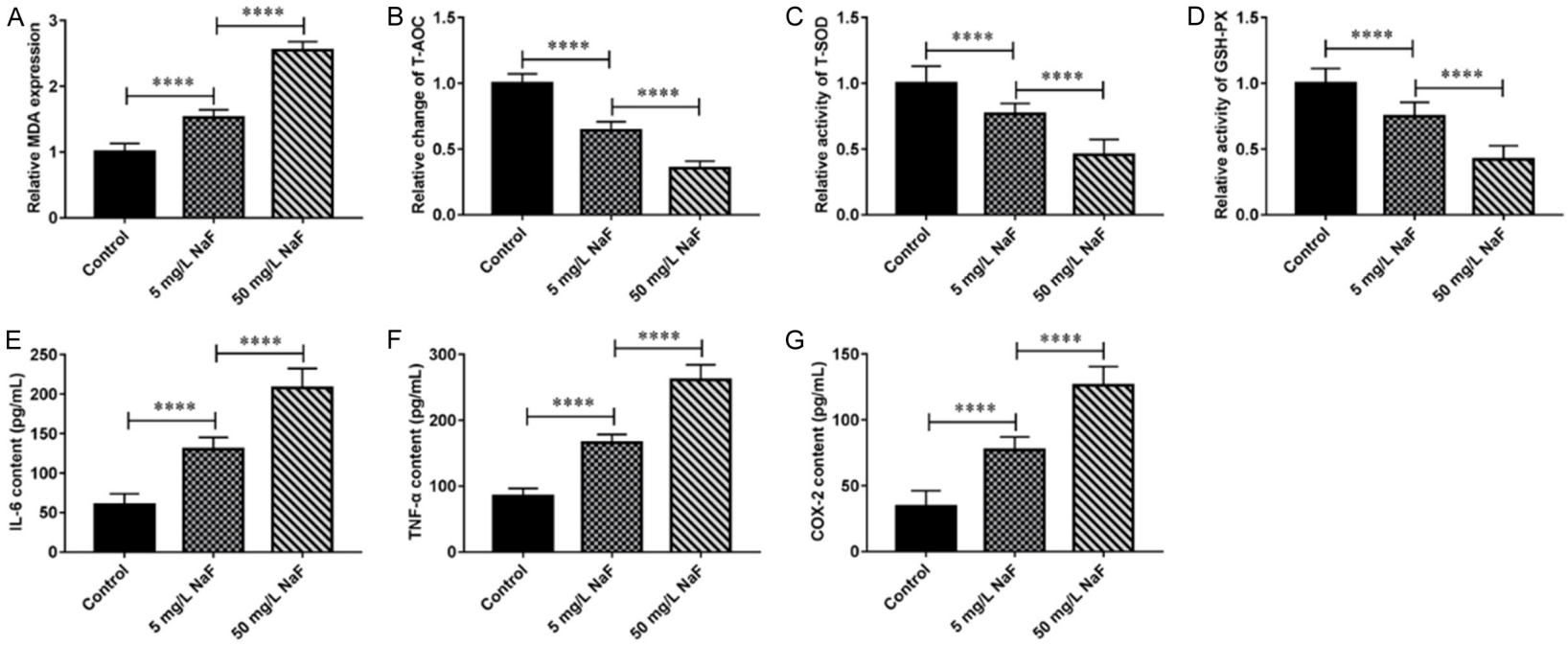

Figure 3. Effects of fluoride exposure on oxidative stress and inflammatory response of chondrocytes. Chondrocytes were exposed to NaF solution (5 mg/L and 50 mg/L). A. Malondialdehyde (MDA) content. B. The levels of total antioxidant capacity (T-AOC). C, D. Activity of total superoxide dismutase (T-SOD) and glutathione peroxidase (GSH-PX). E-G. Secretion levels of inflammatory factors interleukin-6 (IL-6), tumor necrosis factor-α (TNF-α), and cyclooxygenase-2 (COX-2). N=3. ****P<0.01.

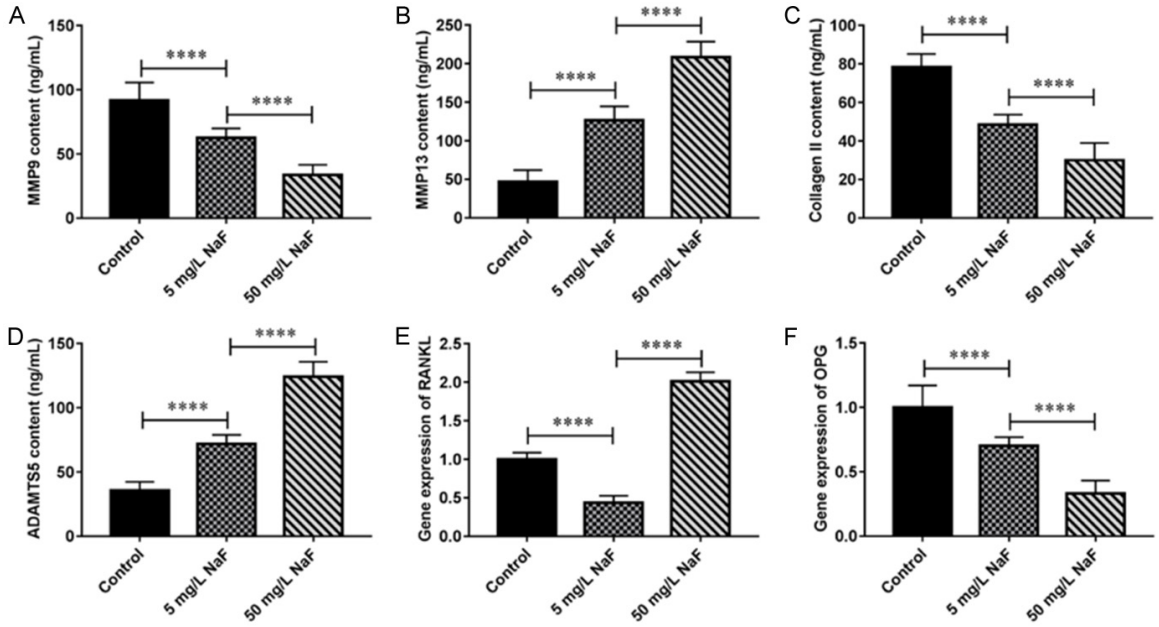

Figure 4. Effects of fluoride exposure on chondrocyte matrix degradation and osteoblast phenotype gene expression. Chondrocytes and osteoblasts were exposed to NaF solution (5 mg/L and 50 mg/L) for 48 h. A. Matrix metalloproteinase-9 (MMP9) content in chondrocytes. B. MMP13 content in chondrocytes. C. Collagen II content in chondrocytes. D. A disintegrin and metalloproteinase with thrombospondin motifs 5 (ADAMTS5) content in chondrocytes. E, F. mRNA expression of receptor activator of nuclear factor κB ligand (RANKL) and osteoprotegerin (OPG) in osteoblasts (RT-qPCR). N=3. ****P<0.01.

low concentration and high concentration of NaF promoted the secretion levels of inflammatory factors IL-6 (**Figure 3E**), TNF-α (**Figure 3F**) and COX-2 (**Figure 3G**), with the higher concentration showing more pronounced effects.

Fluoride exposure promoted chondrocyte matrix degradation and inhibited osteoblast phenotype gene expression

After 48 h exposure to different concentrations of NaF, compared to the control group, the secretion levels of MMP9 (**Figure 4A**) and Collagen II (**Figure 4C**) in chondrocytes of the NaF exposure group were decreased, while the secretion levels of MMP13 (**Figure 4B**) and ADAMTS5 (**Figure 4D**) were increased, and these changes were dose-dependent. Additionally, the expression of RANKL in osteoblasts in the low concentration group was significantly decreased; however, the expression of RANKL in osteoblasts in the high concentration group was significantly increased (**Figure 4E**). Compared to the control group, the expression of OPG in osteoblasts of low- and high-concentration groups was significantly decreased, with a dose-dependent decline observed (**Figure 4F**).

Fluorosis accelerated cartilage injury in rats

In the control group, we observed that the lower incisors of rats were brownish-yellow, with translucent enamel and a glossy surface. In the low fluoride group, the rats' teeth showed yellow and white discoloration, with chalky stripes of varying degrees, but still retained some luster. In the high fluoride group, the teeth appeared dull, with chalky white markings, and some teeth had small grooves, cracks, or even defects (**Figure 5A**). Fluoride exposure significantly increased the levels of both urinary fluoride (**Figure 5B**) and bone fluoride (**Figure 5C**). H&E staining results showed notable changes in cartilage tissue. In the control group, the cartilage layer was thicker, with small cells arranged in a single layer at the periphery and larger, columnar cells toward the center, with a clear boundary separating the cartilage from the bone. In contrast, in the fluoride-exposed groups, the cartilage layer became thinner, with fewer chondrocytes and disorganized cellular arrangement (**Figure 5D**, **5E**). TRAP staining showed the presence of osteoclasts in the cartilage tissue of both low and high fluoride exposure groups. These osteoclasts exhibited abun-

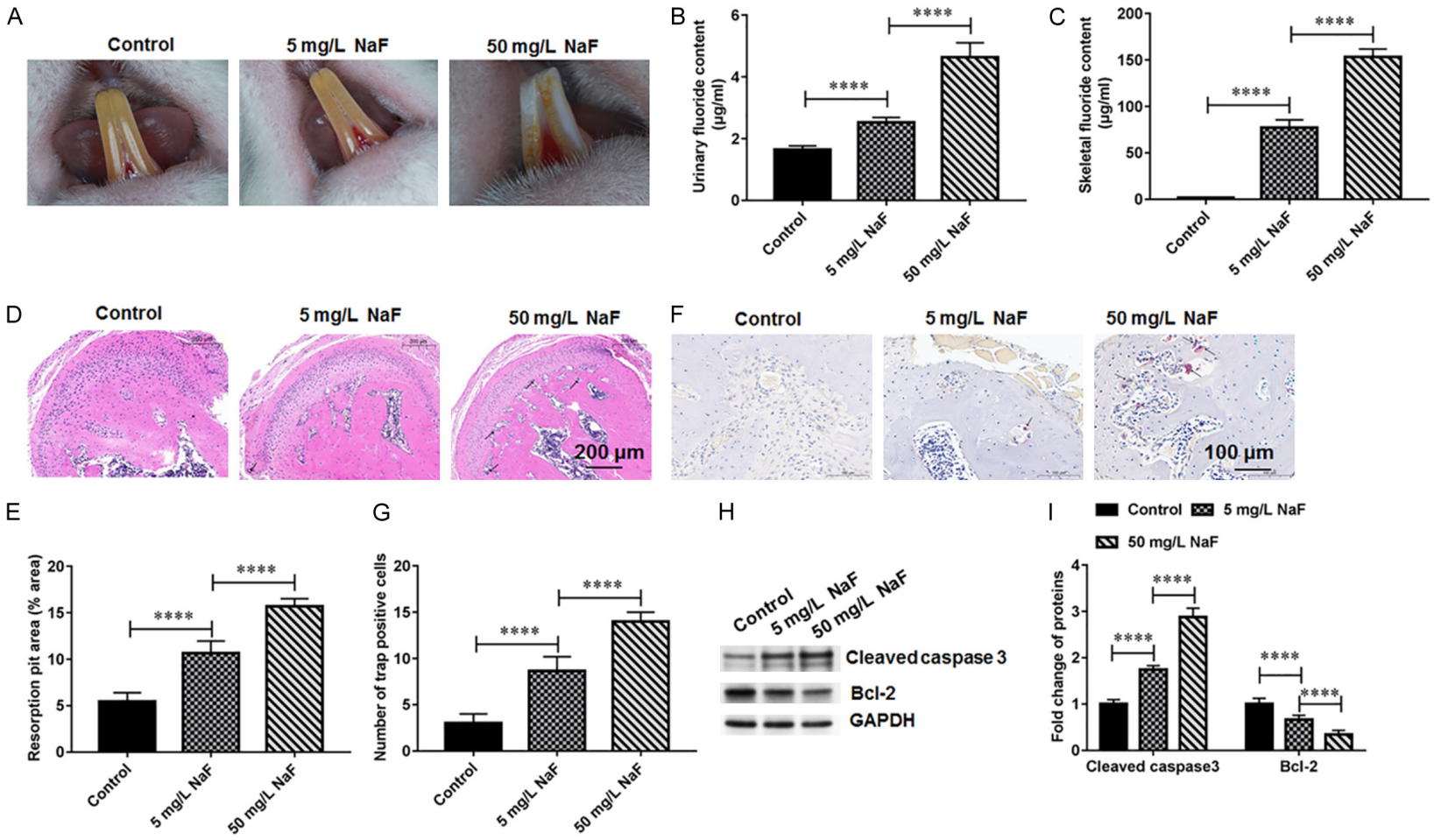

Figure 5. Effects of fluoride exposure on condylar cartilage tissue in rat model. Rats were given 5 mg/L and 50 mg/L NaF solution for 3 months to establish a rat model of fluorosis. A. Representative images of rat lower incisors after NaF administration for three months. B. Urinary fluoride content. C. Skeletal fluoride content. D, E. Representative images of condylar cartilage tissue (H&E staining). F, G. Representative images of osteoclasts in condylar cartilage tissue (TRAP staining). H, I. Protein expression of Cleaved caspase 3 and Bcl-2. N=3. ****P<0.01.

dant cytoplasm, multinucleation, and irregular morphology. A significantly higher number of osteoclasts was observed in the high fluoride group compared to the low fluoride group (**Figure 5F**, **5G**). In addition, WB results showed that compared with the control, the expression of cleaved caspase 3 protein increased, and Bcl-2 protein decreased in cartilage tissue from fluoride groups, both of which were dose-dependent (**Figure 5H**, **5I**).

Discussion

Fluorine is widely distributed in nature as fluoride. Long-term intake of fluorine through water, food and air leads to excessive aggregation of fluorine in the human body, potentially causing fluorosis [13]. It is estimated that approximately 100 million people worldwide suffer from dental and bone damage due to the consumption of fluoride-rich groundwater [14]. Fluorine-induced damage affects bones and cartilage, with current studies research primarily focusing on extremities and the spine. As the incidence of temporomandibular disorder (TMD) syndrome continues to rise in patients with dental fluorosis, research focused on the effects of fluorine on the temporomandibular joint (TMJ). The condylar process, an important bony structure involved in the TMJ movement, is also vulnerable to fluoride. This study initially explored the effects of fluoride on condylar cartilage and subchondral bone.

In this study, 3-week-old SD rats were selected for modeling. Male rats were selected because sex hormones can influence early bone microstructural changes during fluoride exposure, and significant differences in damage occur at high fluoride concentrations. Over time, all rats from the experimental group developed different degrees of dental fluorosis after 3 months of fluoride exposure, indicating that fluoride accumulation had reached levels sufficient to induce toxicity. Our results align with previous studies. For example, Feltrin et al. found that rats exposed to fluoride or fluoride combined with amoxicillin developed dental fluorosis, while exposure to amoxicillin alone did not cause enamel defects [15]. Another study showed that the severity of dental fluorosis in rats exposed to fluoride for 1 and 3 months was significantly correlated with oxidative stress marker MDA [16].

Osteoclasts play an important role in bone resorption and remodeling. These multinucleated giant cells are formed by the fusion of mononuclear macrophages. H&E staining revealed the presence of osteoclasts in condylar subchondral bones of the LF and HF groups. TRAP further showed that compared to the LF group, the number of osteoclasts significantly increased in the HF group, indicating that high-concentration fluoride may promote bone resorption in condylar subchondral bones.

To further investigate the mechanism of fluoride's action on the condylar process, we cultured condylar chondrocytes and subchondral osteoblasts *in vitro*. CCK-8 assays demonstrated that high fluoride concentrations decreased the cellular viability of chondrocytes and osteoblasts. Longer exposure to fluorine resulted in more significant inhibition of cellular proliferation. However, low-concentration fluoride promoted cellular proliferation, indicating that fluorine could either upregulate or downregulate proliferation depending on concentration.

Analysis of MMP9 and MMP13 expression revealed that fluorine at different concentrations downregulated MMP9 expression, while high-concentration fluorine enhanced MMP13 expression. In studies on bone-related genes in osteofluorosis, MMP9 and MMP13 have been identified as key regulators in fluorine-induced inflammation and apoptosis of osteoclasts and chondrocytes [17]. Both MMP9 and MMP13 belong to the matrix metalloproteinase family, with MMP9 involved in degrading and remodeling the extracellular matrix, and MMP13 playing a critical role in the destruction of articular cartilage by cleaving type II collagen [18, 19]. These findings suggest that fluoride disrupts the dynamic balance of the extracellular matrix and accelerates chondrocyte aging, degeneration, and inflammatory lesions.

RANKL is vital in regulating osteoclast activation, differentiation, and maturation during bone remodeling. OPG inhibits osteoclast differentiation and bone resorption. RANKL and OPG can synergistically trigger osteoclast apoptosis, with its onset and degree depending on the ratio of RANKL to OPG. In our experiments, low-concentration fluorine inhibited RANKL and OPG expression, while high-concentration fluorine promoted RANKL expression. In the case of low-concentration fluorine,

osteoblasts inhibited osteoclast bone absorption, while in the case of high-concentration fluorine, the RANKL/OPG ratio was increased by upregulating RANKL, thus stimulating osteoclastogenesis and causing bone resorption. It was reported that in fluoride-exposed ovariectomized rats, the levels of bone alkaline phosphatase and tartrate resistant acid phosphatase increased, and the number of osteoclasts rose due to activation of the RANKL/RANK/OPG signaling pathway [20]. Another study showed that parathyroid hormone enhanced the effect of fluoride on the osteoclastogenesis-related molecules, with significant increases in the gene expression levels of TRAP and RANK in osteoclast precursors co-cultured with osteocyte-like cells exposed to fluoride [21]. All these findings show that fluoride exposure increases osteoclasts and leads to bone resorption. However, because MMP, OPG, and RANKL expression are regulated by various signaling factors, the specific mechanism of their effects needs investigation in future studies.

Conclusion

Fluorine induces pathologic changes in condylar processes and exerts bidirectional modulating effects on condylar cartilage and subchondral bones. By influencing the expression of MMP, RANKL, and OPG, fluorine regulates osteoclast differentiation and maturation, thereby altering the direction of bone remodeling. While this study sheds light on the effect of fluoride on bone remodeling, several limitations remain. The sample size of experimental animals is small, and the fluoride concentration groups are relatively simple. Future studies will expand the sample size, include a broader range of fluoride concentrations, and explore additional signaling pathways through which fluoride affects cartilage and subchondral bone.

Acknowledgements

Especially, we thank our partner (Yuxiang Yan, Yuting Wang, Doudou Zheng, Nana Lu) for feeding the rats during the experiment.

Disclosure of conflict of interest

None.

Address correspondence to: Qingsong Jiang, Department of Prosthodontics, Beijing Stomatological Hospital, Capital Medical University, Beijing 100050, China. E-mail: qsjiang@ccum.edu.cn

References

[1] Srivastava S and Flora SJS. Fluoride in drinking water and skeletal fluorosis: a review of the global impact. Curr Environ Health Rep 2020; 7: 140-146.

[2] Hung M, Hon ES, Mohajeri A, Moparthi H, Vu T, Jeon J and Lipsky MS. A national study exploring the association between fluoride levels and dental fluorosis. JAMA Netw Open 2023; 6: e2318406.

[3] Podgorski J and Berg M. Global threat of arsenic in groundwater. Science 2020; 368: 845-850.

[4] Wang Y, Li J, Ma T, Xie X, Deng Y and Gan Y. Genesis of geogenic contaminated groundwater: as, F and I. Crit Rev Environ Sci Technol 2020; 51: 2895-2933.

[5] WHO Guidelines Approved by the Guidelines Review Committee, in Guidelines for drinking-water quality: Fourth edition incorporating the first and second addenda. 2022, World Health Organization© World Health Organization 2022.: Geneva.

[6] Podgorski J and Berg M. Global analysis and prediction of fluoride in groundwater. Nat Commun 2022; 13: 4232.

[7] Helte E, Donat Vargas C, Kippler M, Wolk A, Michaëlsson K and Åkesson A. Fluoride in drinking water, diet, and urine in relation to bone mineral density and fracture incidence in postmenopausal women. Environ Health Perspect 2021; 129: 47005.

[8] Umer MF. A systematic review on water fluoride levels causing dental fluorosis. Sustainability 2023; 15.

[9] Strużycka I, Olszewska A, Bogusławska-Kapała A, Hryhorowicz S, Kaczmarek-Ryś M, Grabarek BO, Staszkiewicz R, Kuciel-Polczak I and Czajka-Jakubowska A. Assessing fluorosis incidence in areas with low fluoride content in the drinking water, fluorotic enamel architecture, and composition alterations. Int J Environ Res Public Health 2022; 19: 7153.

[10] Zhou J, Sun D and Wei W. Necessity to pay attention to the effects of low fluoride on human health: an overview of skeletal and non-skeletal damages in epidemiologic investigations and laboratory studies. Biol Trace Elem Res 2022; 201: 1627-1638.

[11] Januzzi M, Neto CM, Moreno A, dos Santos E, de Caxias F, da Silva E, de Athayde F, Volce AS, Rodrigues A, Dela Líbera J and Turcio J. Relationship between self-reported pain, pain threshold, pain catastrophization and quality

of life in patients with TMD. J Clin Exp Dent 2023; 15: e23-e31.
[12] Nagappan N, Tirupati N, Gopinath NM, Selvam DP, Subramani GP and Subbiah GK. Oral Health Status of sports university students in Chennai. J Pharm Bioallied Sci 2019; 11 Suppl 2: S180-S183.
[13] Alarcón-Herrera MT, Martin-Alarcon DA, Gutiérrez M, Reynoso-Cuevas L, Martín-Domínguez A, Olmos-Márquez MA and Bundschuh J. Co-occurrence, possible origin, and health-risk assessment of arsenic and fluoride in drinking water sources in Mexico: geographical data visualization. Sci Total Environ 2020; 698: 134168.
[14] Joseph A, Rajan R, Paul J, Cherian KE, Kapoor N, Jebasingh F, Shyamsunder Asha H, Thomas N and Paul TV. The continuing crippling challenge of skeletal fluorosis - case series and review of literature. J Clin Transl Endocrinol Case Rep 2022; 24.
[15] Feltrin-Souza J, Costa SAD, Bussaneli DG, Santos-Pinto L, Cerri PS, Cury J, Tenuta L and Cordeiro RCL. In vivo effect of fluoride combined with amoxicillin on enamel development in rats. J Appl Oral Sci 2021; 29: e20210171.
[16] Zhong N, Yao Y, Ma Y, Meng X, Sowanou A and Pei J. Effects of fluoride on oxidative stress markers of lipid, gene, and protein in rats. Biol Trace Elem Res 2021; 199: 2238-2246.
[17] Wang M, Luo K, Sha T, Li Q, Dong Z, Dou Y, Zhang H, Zhou G, Ba Y and Yu F. Apoptosis and inflammation involved with fluoride-induced bone injuries. Nutrients 2024; 16: 2500.
[18] Francisco V, Ait Eldjoudi D, González-Rodríguez M, Ruiz-Fernández C, Cordero-Barreal A, Marques P, Sanz MJ, Real JT, Lago F, Pino J, Farrag Y and Gualillo O. Metabolomic signature and molecular profile of normal and degenerated human intervertebral disc cells. Spine J 2023; 23: 1549-1562.
[19] Teunissen van Manen IJ, van Kooten NJT, Di Ceglie I, Theeuwes WF, Jimenez-Royo P, Cleveland M, van Lent P, van der Kraan PM, Blom AB and van den Bosch MHJ. Identification of CD64 as a marker for the destructive potential of synovitis in osteoarthritis. Rheumatology (Oxford) 2024; 63: 1180-1188.
[20] Jin Y, Zhou BH, Zhao J, Ommati MM, Wang S and Wang HW. Fluoride-induced osteoporosis via interfering with the RANKL/RANK/OPG pathway in ovariectomized rats: oophorectomy shifted skeletal fluorosis from osteosclerosis to osteoporosis. Environ Pollut 2023; 336: 122407.
[21] Jiang N, Guo F, Xu W, Zhang Z, Jin H, Shi L, Zhang X, Gao J and Xu H. Effect of fluoride on osteocyte-driven osteoclastic differentiation. Toxicology 2020; 436: 152429.